# 7 Electromagnetic resonators and filters

## 7.1 INTRODUCTION

At radio frequencies tuned circuits are used to provide frequency selectivity. Resonant elements are used for similar purposes at microwave and optical frequencies. They can take many forms but all can be modelled fairly accurately by one of the resonant circuits shown in Fig. 7.1. The impedance of the parallel resonant network (Fig. 7.1(a)) is given by

$$Z = \frac{R}{1 - \mathrm{j}\dfrac{R}{\omega L}(1 - \omega^2 LC)}. \tag{7.1}$$

At microwave frequencies the individual circuit components have no real significance and it is usual to rewrite (7.1) in the form

$$Z = \frac{R}{1 + \mathrm{j}Q\left(\dfrac{\omega}{\omega_0} - \dfrac{\omega_0}{\omega}\right)}, \tag{7.2}$$

where
$$\omega_0 = 1/\sqrt{(LC)} \tag{7.3}$$

and
$$Q = R/\omega_0 L = \omega_0 RC. \tag{7.4}$$

To understand what this expression means let us consider separately the amplitude and phase of $Z$. The amplitude is

$$|Z| = \frac{R}{\left[1 + Q^2\left(\dfrac{\omega}{\omega_0} - \dfrac{\omega_0}{\omega}\right)^2\right]^{\frac{1}{2}}}. \tag{7.5}$$

This expression clearly has a maximum value of $|Z| = R$ when the frequency-dependent term on the bottom line is zero. This occurs at the resonant frequency of the network given by (7.3). At all other frequencies $|Z| < R$.



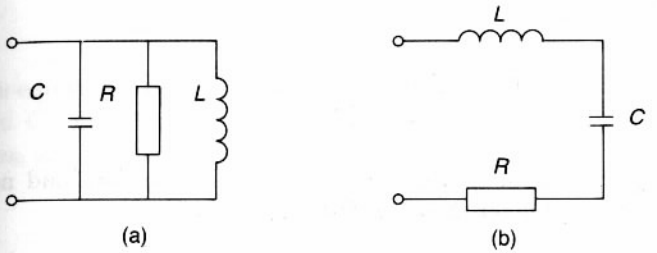


**Fig. 7.1** (a) Parallel and (b) series resonant circuits.

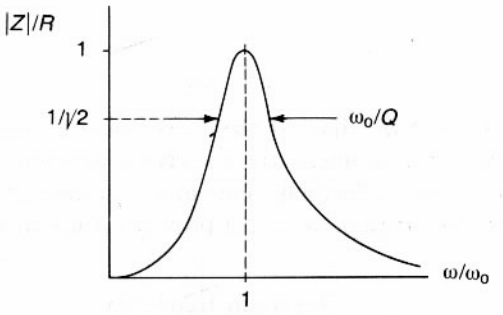


**Fig. 7.2** Amplitude-response curve of a parallel resonant circuit.

Figure 7.2 shows how $|Z|$ varies with frequency. The width of the curve is determined by the parameter $Q$ in (7.2). The relationship is usually expressed in terms of the width of the curve at the 3 dB points. If the circuit is driven by a constant-current source $I$ then the voltage across it can be expressed in decibels normalized to the peak value as

$$20 \log_{10}\left(\frac{|Z|I}{RI}\right). \tag{7.6}$$

This expression has a value of $-3$ dB when $|Z| = R/\sqrt{2}$ and then, from (7.5),

$$1 + Q^2\left(\frac{\omega}{\omega_0} - \frac{\omega_0}{\omega}\right)^2 = 2. \tag{7.7}$$

The width of the curve is usually small so we can write

$$\omega = \omega_0 + \delta\omega,$$

where $\delta\omega \ll \omega_0$. Then, from (7.7),

$$\frac{\omega}{\omega_0} - \frac{\omega_0}{\omega} = \pm\frac{1}{Q} \tag{7.8}$$

so that

$$\left(1 + \frac{\delta\omega}{\omega_0}\right) - \frac{1}{\left(1 - \frac{\delta\omega}{\omega_0}\right)} = \pm\frac{1}{Q}. \tag{7.9}$$

Expanding the second bracket by the binomial theorem and neglecting powers of $\delta\omega/\omega_0$ higher than the first gives

$$\left(1 + \frac{\delta\omega}{\omega_0}\right) - \left(1 - \frac{\delta\omega}{\omega_0}\right) = \pm\frac{1}{Q} \tag{7.10}$$

or

$$\delta\omega \simeq \pm\frac{\omega_0}{2Q} \tag{7.11}$$

so that the width of the curve at the 3 dB points is $\omega_0/Q$ as shown in Fig. 7.2. Modern test equipment can display the response curve as shown with the vertical scale in decibels. This makes it easy to measure the $Q$ factor of a resonator. Equation (7.11) provides a useful definition of the $Q$ factor as

$$Q = \frac{\text{Resonant frequency}}{\text{Bandwidth}}. \tag{7.12}$$

Consideration of Fig. 7.1(a) and (7.4) shows that to obtain a high $Q$ factor we must have a high shunt resistance. At radio frequencies resonant circuits made with lumped components generally have $Q$ factors of the order of a few hundred. Microwave resonators commonly have $Q$ factors of 1000 and can be made with values as high as 30 000 by careful design and manufacture. From these considerations it is evident that a high $Q$ factor implies low losses and that leads to another useful way of defining $Q$.

When an alternating voltage $V = V_0 \exp j\omega t$ is applied to the terminals of the circuit shown in Fig. 7.1(a) the stored energy is

$$W_E = \tfrac{1}{2}CV_0^2. \tag{7.13}$$

It can be shown that this energy is transferred backwards and forwards between the capacitor and the inductor during each cycle with the total stored energy remaining constant provided that the voltage at the terminals is held constant. The mean rate of dissipation of energy is

$$P_L = V_0^2/2R. \tag{7.14}$$

Substituting these expressions into (7.4) gives

$$Q = \omega_0 W_E/P_L. \tag{7.15}$$

This equation can also be expressed as



$$Q = \frac{2\pi \times \text{Stored energy}}{\text{Energy dissipated per cycle}}. \tag{7.16}$$

The basic equivalent circuit of Fig. 7.1(a) is defined by the three parameters $R$, $L$ and $C$. So far we have only generated two alternative parameters namely $\omega_0$ and $Q$. The third is defined from (7.4) as

$$\left(\frac{R}{Q}\right) = \sqrt{\left(\frac{L}{C}\right)}. \tag{7.17}$$

Note that the value of $(R/Q)$ is independent of the losses in the resonator. The physical significance of this parameter is revealed by substituting from (7.14) into (7.15) to give

$$\left(\frac{R}{Q}\right) = \frac{V_0^2}{2\omega_0 W_E}. \tag{7.18}$$

Thus $(R/Q)$ is a measure of the relationship between the voltage across the resonator and the stored energy. In free-electron devices such as klystrons and particle accelerators the voltage across a resonator is used to interact with charged particles. A high $(R/Q)$ means a high interaction voltage for a given stored energy so this parameter is a useful figure of merit.

To complete our review of the theory of parallel resonant circuits we must examine the phase of Z. From (7.2) we have

$$\angle Z = \arctan\left[Q\left(\frac{\omega_0}{\omega} - \frac{\omega}{\omega_0}\right)\right]. \tag{7.19}$$

This expression is zero at resonance so that $Z$ is then wholly real as is clear from (7.2). As $\omega$ tends to zero the behaviour is dominated by the reactance of the inductor and $\angle Z$ tends to 90°. As $\omega$ tends to infinity the capacitor has the greater effect and $\angle Z$ tends to −90°. This behaviour is summarized in Fig. 7.3. The phase reversal at resonance is an important feature of the behaviour of any resonant device.

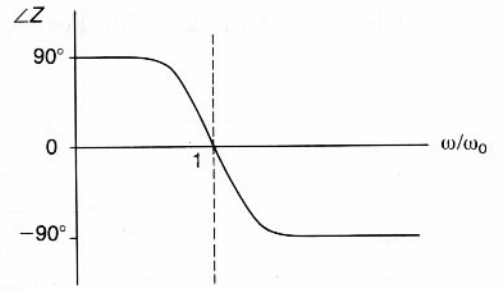


**Fig. 7.3** Phase response curve of a parallel resonant circuit.

The properties of the series resonant circuit shown in Fig. 7.1b can be revealed by a similar analysis. The impedance of the network is

$$Z = R + j\omega L + \frac{1}{j\omega c} \tag{7.20}$$

which can be written

$$Z = R\left[1 + jQ\left(\frac{\omega}{\omega_0} - \frac{\omega_0}{\omega}\right)\right] \tag{7.21}$$

where

$$\omega_0 = 1/\sqrt{(LC)} \quad \text{and} \quad Q = \frac{1}{\omega_0 RC}. \tag{7.22}$$

This can be written, alternatively, as an admittance

$$Y = \frac{G}{1 + jQ\left(\frac{\omega}{\omega_0} - \frac{\omega_0}{\omega}\right)}, \tag{7.23}$$

where $G = 1/R$. Equation (7.23) is mathematically identical to (7.2) so all the conclusions for parallel resonant circuits can be applied to series resonant circuits if admittance is substituted for impedance. Hence a series resonant circuit has a maximum admittance $G$ at resonance and a phase reversal exactly as shown in Figs. 7.2 and 7.3.

## 7.2 TRANSMISSION-LINE RESONATORS

In distributed circuits such as transmission lines and waveguides resonant behaviour is associated with the presence of standing waves. To illustrate this consider the three situations shown in Fig. 7.4. Figure 7.4(a) shows a length of transmission line with short circuits at either end. A voltage wave is reflected by a short circuit with 180° change of phase. If a wave starts from A with zero phase it has a phase of $-\theta$ on arrival at B. The reflected wave at B has a phase of $(\pi - \theta)$ which becomes $(\pi - 2\theta)$ on arrival at A. This wave after reflection has a phase of $(2\pi - 2\theta)$. For resonance to occur

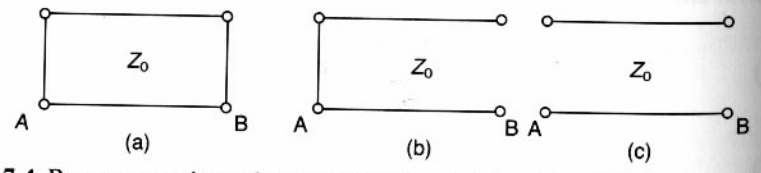


**Fig. 7.4** Resonant sections of transmission line: (a) short circuit both ends, (b) short circuit and open circuit, and (c) open circuit both ends.



it is necessary for this wave to be in phase with the wave originally launched at A. The condition for resonance is therefore

$$(2\pi - 2\theta) = 0, -2\pi, -4\pi, \ldots, \text{etc.},$$

that is

$$\theta = n\pi, \tag{7.24}$$

where $n$ is a positive integer. In other words the line is resonant when it is a whole number of half wavelengths long.

In the second case shown in Fig. 7.4(b) we recall that a voltage wave is reflected without change of phase by an open circuit. The phase of the wave which has been reflected at both B and A is therefore $(\pi - 2\theta)$. The condition for resonance is therefore

$$(\pi - 2\theta) = 0, -2\pi, -4\pi, \ldots, \text{etc.}$$
$$\theta = (n - \tfrac{1}{2})\pi, \tag{7.25}$$

so the line is an odd number of quarter wavelengths long at resonance.

In the third case the wave is reflected without a change of phase so that for resonance

$$2\theta = 2\pi, 4\pi, \ldots, \text{etc.}$$
$$\theta = n\pi \tag{7.26}$$

giving the same frequencies as in the first case.

The wave patterns on the lines are given by the sums of waves of equal amplitudes travelling in the positive and negative directions.

$$V = V_0 \exp j(\omega t - kx) \pm V_0 \exp j(\omega t + kx). \tag{7.27}$$

The sign of the amplitude of the wave travelling in the $-x$ direction is chosen so that the boundary condition at A is satisfied. Thus when there is an open circuit at A

$$V = 2V_0 \exp j\omega t \cos kx, \tag{7.28}$$

whilst with a short circuit at A

$$V = -2jV_0 \exp j\omega t \sin kx. \tag{7.29}$$

If the length of the line is $L$ then the boundary conditions at B are satisfied if $\theta = kL$ is given by (7.24) when the two boundaries are the same and by (7.25) when they are different.

The voltage wave patterns at resonance are therefore

$$V = -2jV_0 e^{j\omega t} \sin\left(\frac{n\pi x}{L}\right) \tag{7.30}$$

$$V = -2jV_0 e^{j\omega t} \sin\left(\frac{(n-\frac{1}{2})\pi x}{L}\right) \tag{7.31}$$

and

$$V = 2V_0 e^{j\omega t} \cos\left(\frac{n\pi x}{L}\right), \tag{7.32}$$

for the resonators shown in Fig. 7.4(a), (b) and (c), respectively, where $n = 1, 2, 3$, etc. Note that these are all standing waves, not travelling waves.

This discussion highlights one important difference between a lumped-element resonant circuit and a distributed resonant circuit. That is that a distributed resonant circuit has not one but an infinite set of resonances. Figure 7.5 shows the voltage wave patterns for the lowest three resonant modes of the lines in Fig. 7.4.

**Example**

Calculate the three lowest resonant frequencies for a 1 metre length of polythene insulated coaxial cable with both open- and short-circuit terminations.

*Solution*

The relative permittivity of polythene is 2.25 so the phase velocity is

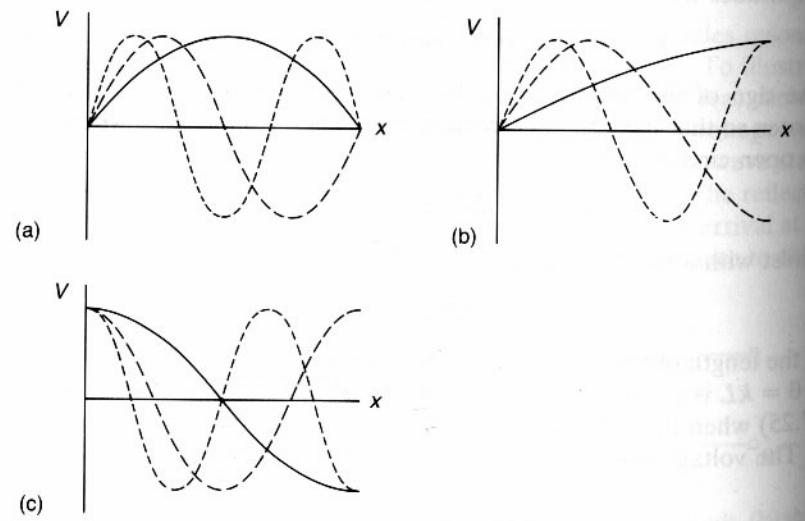


**Fig. 7.5** Voltage standing waves for the lowest three resonances of each of the resonant transmission lines shown in Fig. 7.4.



$c/\sqrt{2.25} = 0.2 \times 10^9\,\mathrm{m\,s^{-1}}$. For an open circuit at one end and a short circuit at the other the resonant frequencies are given by

$$f = (n + \tfrac{1}{2})(v_{ph}/2L) \tag{7.33}$$

so there are resonances at 50 MHz, 150 MHz and 250 MHz. Similarly when there are short or open circuit terminations at both ends the resonant frequencies are

$$f = nv_{ph}/2L \tag{7.34}$$

giving resonances at 100 MHz, 200 MHz and 300 MHz.

This example makes the point that the lowest resonant frequencies of the lengths of cable commonly used in the laboratory are well down into the VHF and UHF regions. Thus if care is not taken with making correct terminations it is possible for resonances in circuits to be troublesome at quite low frequencies. It must be remembered that the sets of resonant frequencies are infinite so resonances can be detected in all higher-frequency bands.

---

The current waveform corresponding to (7.27) is given by

$$I = \frac{V_0}{Z_0} e^{j(\omega t - kx)} \mp \frac{V_0}{Z_0} e^{j(\omega t + kx)}, \tag{7.35}$$

where the reversal of the sign of the second term is necessary because the current in the wave travelling in the negative $x$ direction must be opposite to that for the wave in the positive $x$ direction. The current patterns corresponding to (7.30) to (7.32) are therefore

$$I = \frac{2V_0}{Z_0} e^{j\omega t} \cos\left(\frac{n\pi x}{L}\right) \tag{7.36}$$

$$I = \frac{2V_0}{Z_0} e^{j\omega t} \cos\left[\frac{(n-\frac{1}{2})\pi x}{L}\right] \tag{7.37}$$

$$I = \frac{-2jV_0}{Z_0} e^{j\omega t} \sin\left(\frac{n\pi x}{L}\right). \tag{7.38}$$

Note that the currents and voltages are in phase quadrature in time implying that there is no net power flow in the resonator, also that they are in phase quadrature in space so that a voltage maximum corresponds to a current zero and vice versa. This must be clearly distinguished from the situation with a propagating wave where the current and voltage are in phase.

The voltage and current patterns are associated with distributions of the electric and magnetic fields around the line. Figure 7.6 shows how the field patterns change during one cycle. One way of thinking about this process is to imagine a static charge distribution set up as shown in Fig. 7.6(a). This

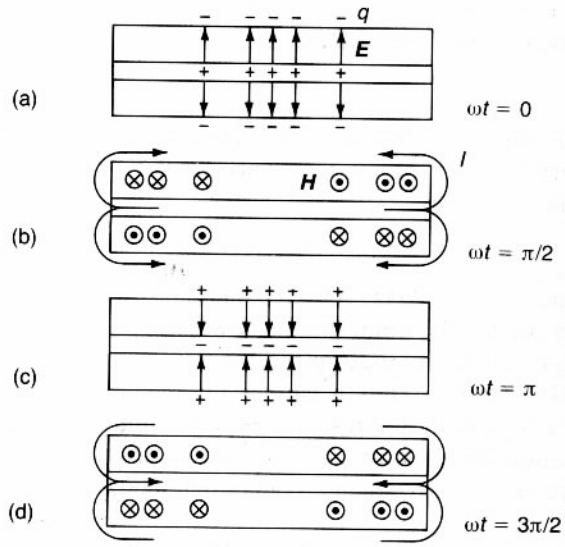


**Fig. 7.6** Resonant section of coaxial line showing the fields, currents and charges at different times during the r.f. cycle.

distribution has an electric field associated with it as shown. The arrangement is unstable and so the positive and negative charges move towards each other producing currents and magnetic fields as shown in Fig. 7.6(b). Because the electrons possess inertia they overshoot producing a new charge distribution as in Fig. 7.6(c). This in turn is unstable and the cycle is continued.

So far we have assumed that the voltages and currents necessary to sustain the oscillation exist without saying how this might be achieved. The resonator shown in Fig. 7.6 is closed and ohmic damping would reduce the magnitude of the oscillation to zero over a few cycles. It follows that any resonator must be coupled to an external power source if sustained oscillation is to occur. The amplitude of oscillation excited is then just that for which the losses exactly match the incoming power.

Figure 7.7 shows a resonant circuit excited from a source of impedance $Z_0$ through a coupling capacitor. At resonance the impedance of the resonant circuit is just $R$ and the output voltage is

$$V_{\text{out}} = \frac{RZ_0 I_0}{Z_0 + R + \mathrm{j}X} \tag{7.39}$$

using the current-splitting rule. The amplitude of the output voltage is greatest when $X = 0$ but then $Z$ appears in parallel with $R$ lowering the $Q$ of the resonator. The loaded $Q$ of the resonator is



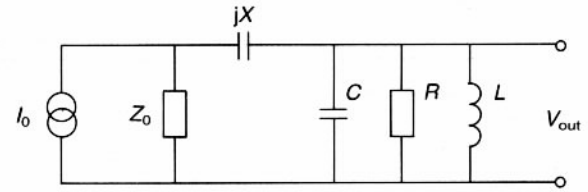


**Fig. 7.7** Equivalent circuit of a parallel resonant circuit capacitively coupled to a source.

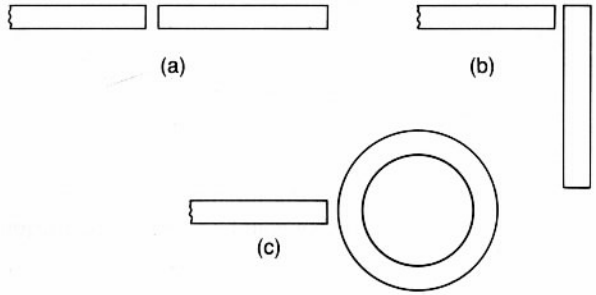


**Fig. 7.8** Microstrip resonators: (a) end-coupled, (b) side-coupled, and (c) ring resonators.

$$Q_{\text{L}} = \frac{1}{\omega_0 L}\left(\frac{RZ_0}{R + Z_0}\right), \tag{7.40}$$

where $Z_0$ is the impedance of the external loading of the resonator. Since one of the main uses of resonators is to provide frequency selectivity it is usually undesirable to allow the $Q$ to be degraded in this way. Thus the coupling between the input line and the resonator is usually weak and $X$ is correspondingly large.

The circuit of Fig. 7.7 is equivalent to the microstrip resonators shown in Fig. 7.8. The straight resonators shown in Figs. 7.8(a) and (b) must have lengths slightly less than half a wavelength to allow for the effects of fringing discussed in Section 6.2. The ring resonator must have a perimeter equal to one wavelength. The ring resonator has the advantage that it has a higher $Q$ factor because it does not have the radiation losses which occur at the free ends of the straight resonators. A fuller discussion of microstrip resonators is given by Edwards (1981).

Coupling into the coaxial-line resonator shown in Fig. 7.6 can be achieved by means of an electric dipole at its mid-plane or a magnetic dipole at the end. These could be either wire or aperture dipoles. Figure 7.9 shows coupling arrangements with wire dipoles. The electric dipole (Fig. 7.9(a)) is placed at the plane of maximum electric field for optimum coupling. The equivalent circuit of this arrangement is as shown in Fig. 7.7. The magnetic

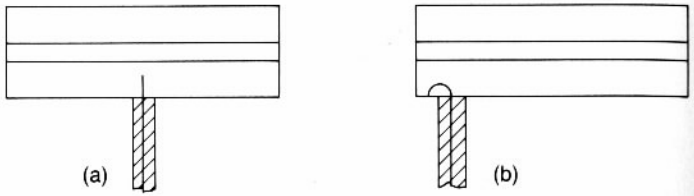


**Fig. 7.9** Coupling into a coaxial-line resonator: (a) via the electric field, and (b) via the magnetic field.

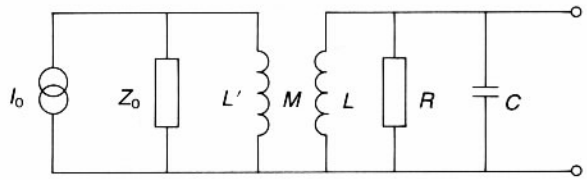


**Fig. 7.10** Equivalent circuit for inductive coupling to a parallel resonant circuit.

dipole (Fig. 7.9(b)) is placed in a region of high magnetic field. The equivalent circuit of this arrangement is shown in Fig. 7.10. The strength of the coupling is adjusted by changing the size of the coupling loop or by turning so that it intercepts less of the flux circulating in the resonator. Either of these is equivalent to adjusting the mutual inductance $M$ in Fig. 7.10. To couple selectively into a higher-order mode of the resonator the dipole is moved to a position which corresponds to a field maximum for that mode.

## 7.3 CAVITY RESONATORS

We have seen in Chapter 2 that metallic waveguides can be treated as transmission lines. It follows that resonators can be made out of short-circuited sections of waveguide. Open-circuit terminations are impossible to realize because an open end of waveguide radiates too well. For the moment let us consider only TE modes in the rectangular waveguide shown in Fig. 7.11. The electric fields for these modes are given by (2.60) and (2.61). The $z$ variation is as exp j($\omega t - k_g z$), where

$$\left(\frac{n\pi}{a}\right)^2 + \left(\frac{m\pi}{b}\right)^2 + k_g^2 = k_0^2 \tag{7.41}$$

(equation (2.63)). When the ends of the waveguide are closed by metal walls separated by a distance $c$ the boundary conditions in the $z$ direction require that

$$k_g c = l\pi, \tag{7.42}$$



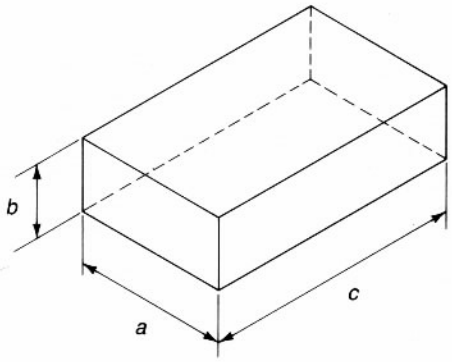


**Fig. 7.11** Rectangular resonant cavity.

where $l = 1, 2, 3$, etc. Substituting this into (7.41) we find that the resonant frequencies are given by

$$\frac{\omega_0}{v_{ph}} = \left[\left(\frac{n\pi}{a}\right)^2 + \left(\frac{m\pi}{b}\right)^2 + \left(\frac{l\pi}{c}\right)^2\right]^{\frac{1}{2}}, \tag{7.43}$$

where $v_{ph}$ is the phase velocity of TEM waves in the medium filling the waveguide. When the field patterns of these modes are analysed it is found that the electric and magnetic fields are in phase quadrature in both time and space exactly as in the case of the coaxial-line resonator discussed above. The field patterns for a few of the lower resonant modes are shown in Fig. 7.12. The notation for these resonances is a bit tricky because it depends upon which direction is taken as the reference direction. For example the mode shown in Fig. 7.12(a) could be described as, for example, $TE_{011}$ or $TM_{110}$. It is useful to acquire the ability to sketch the field patterns of different possible resonant modes of a cavity. It helps to think of the magnetic field as being generated by the displacement current associated with the electric field but it has to be remembered that they are in phase quadrature.

The fields of the lowest resonance of an air-filled cavity are given by

$$E_x = E_0 \sin\left(\frac{\pi y}{a}\right) \sin\left(\frac{\pi z}{c}\right) e^{j\omega t} \tag{7.44}$$

$$H_y = \frac{j\pi E_0}{\omega\mu_0 c} \sin\left(\frac{\pi y}{a}\right) \cos\left(\frac{\pi z}{c}\right) e^{j\omega t} \tag{7.45}$$

$$H_z = \frac{-j\pi E_0}{\omega\mu_0 a} \cos\left(\frac{\pi y}{a}\right) \sin\left(\frac{\pi z}{c}\right) e^{j\omega t} \tag{7.46}$$

Integrating the square of the electric field gives the stored energy as

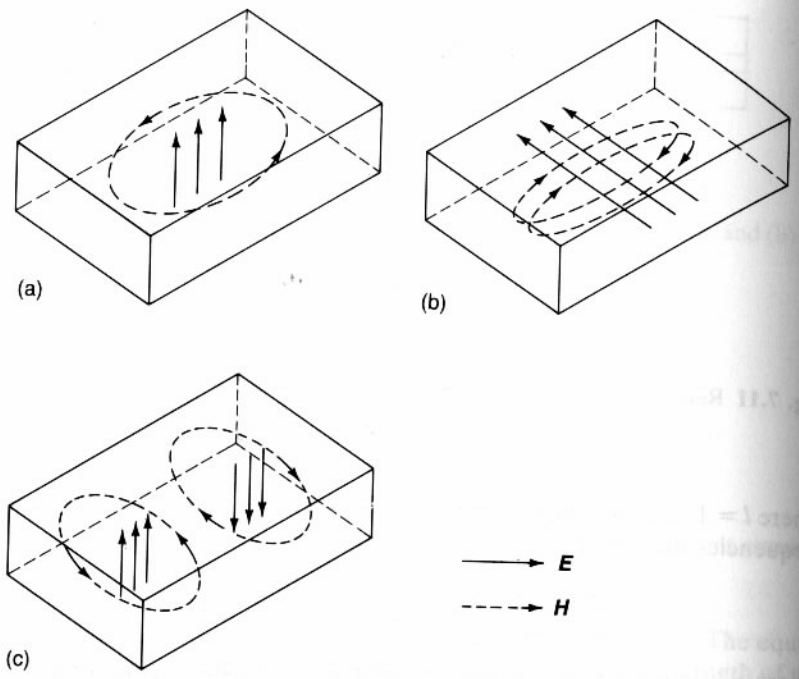


**Fig. 7.12** Modes in a rectangular resonant cavity: (a) $TE_{110}$, (b) $TE_{101}$ and (c) $TE_{210}$.

$$W_E = \frac{\varepsilon_0}{8} abc\, E_0^2, \tag{7.47}$$

whence the $(R/Q)$ of the mode is, from (7.18),

$$\left(\frac{R}{Q}\right) = \frac{4}{\pi}\sqrt{\left(\frac{\mu_0}{\varepsilon_0}\right)}\frac{b}{(a^2 + c^2)^{\frac{1}{2}}}. \tag{7.48}$$

The previous discussion has concentrated on rectangular cavities because they are easiest to analyse mathematically. It must be remembered, however, that any closed conducting box will behave as a resonator with an infinite number of resonant modes. In general the lowest mode will have a wavelength which is of the same order of magnitude as the longest dimension of the box. Circular 'pill box' and re-entrant cavities as shown in Fig. 7.13 are in common use. An analytical solution for the pill-box cavity can be obtained in terms of Bessel functions (Appendix B). The lowest resonant frequency is given by

$$k_0 r = 2.405. \tag{7.49}$$

The $(R/Q)$ depends only on the cavity geometry. It can be computed from (7.6) using the exact solution for the electric field distribution. The result is



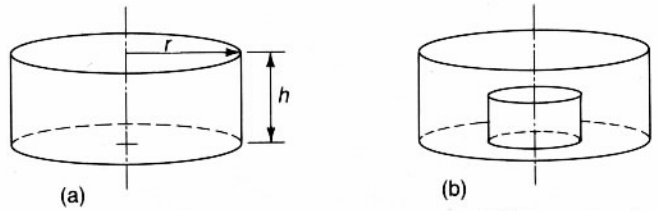


**Fig. 7.13** Cylindrical resonant cavities: (a) pill-box, and (b) re-entrant cavities.

$$\left(\frac{R}{Q}\right) = 188.1\,\frac{h}{r}. \tag{7.50}$$

It is not possible to obtain exact analytical solutions for circular re-entrant cavities. Design curves are given by Saad (1971) and useful approximate formulae by Fujisawa (1958).

For more complicated cavity shapes it is necessary to make use of computer modelling techniques. Examples are the programs SUPERFISH (Halbach and Holsinger, 1976) and URMEL (Weiland, 1983) for cylindrically symmetrical cavities and MAFIA (Weiland, 1985) and TLM (Akhtarzad and Johns, 1975) for general three-dimensional cavity geometries.

In general, computations of cavity $Q$ factors assume that the losses are small so that the current distribution in the walls is the same as that for a lossless cavity. The energy loss per cycle and the stored energy are computer by integrating the current and field distributions and $Q$ is calculated from (7.15). At microwave frequencies the surface roughness is often comparable with the skin depth so the $Q$ of a cavity depends upon surface finish as well as on the material from which the cavity is made. It is then necessary to use figures for surface resistance determined by experiment.

Coupling into cavities is achieved by using electric or magnetic dipoles arranged to couple to field maxima within the cavity exactly as in the case of the coaxial cavity discussed above. Figure 7.14 shows coupling from a waveguide to a cavity through an iris which acts as a magnetic dipole coupling element.

## 7.4 EFFECT OF RESONANCE ON SCREENED ENCLOSURES

We have already noted that electromagnetic power can be coupled into a screened enclosure through any small holes in the screen. The effects of such coupled power are made much worse if it happens to excite one of the resonances of the enclosure.

### Example

Estimate the screening effectiveness of an aluminium box 1.0 mm thick whose dimensions are 50 mm × 100 mm × 200 mm at its lowest resonant

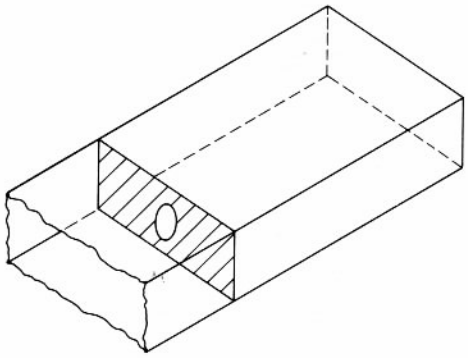

**Fig. 7.14** Coupling from a waveguide to a resonant cavity via an iris.

frequency if there is a hole 5 mm in diameter in one side of the box. Assume that the $Q$ of the resonance is 500.

*Solution*

The lowest resonant frequency of this box is given by (7.43) with $m = n = 1$ and $l = 0$. The result is 1.68 GHz. At this frequency the screening effectiveness of the enclosure without holes in it is very high.

The screening effectiveness of the enclosure can thus be calculated from the leakage through the hole using (6.16), (6.19) and (6.25) so that

$$A_a \simeq 27.3(1/5) = 5.5\,\text{dB} \tag{7.51}$$

$$R_a \simeq -20 \log_{10}\left(\frac{2 \times 5}{179}\right) = 25.1\,\text{dB} \tag{7.52}$$

and

$$B_a \simeq -20 \log_{10}(1 - 10^{-5.5}) = 2.9\,\text{dB} \tag{7.53}$$

so that $S = 33.5$ dB. We recall that this is the ratio of the signal level inside the box to that which would exist if the box were not present. This figure assumes that the box is not resonant. If the power leaking into the box is $P$ (assumed to be spread uniformly over the cross-sectional area of the box) then the mean electric field strength is

$$E_0 = \left[\frac{2PZ_0}{(0.05 \times 0.2)}\right]^{\frac{1}{2}}$$
$$= 275\sqrt{P}. \tag{7.54}$$

When the box is resonant the power is dissipated in the losses in the walls. For the dimensions given $(R/Q) = 26.8$ from (7.48) so that $R = 26.8 \times 500 = 13.4\,\text{k}\Omega$. The voltage across the box is therefore



$$V_0 = E_r \times 0.05$$
$$= (2RP)^{\frac{1}{2}}, \tag{7.55}$$

whence the electric field strength at the centre of the resonant cavity is

$$E_R = 3274\sqrt{P}. \tag{7.56}$$

Comparing (7.54) and (7.56) shows that the effect of the resonance is to produce a substantial increase in the peak value of the electric field inside the box. The reduction in screening effectiveness is

$$S_R = 20 \log_{10}\left|\frac{E_R}{E_0}\right| = 21.5\,\text{dB} \tag{7.57}$$

giving a final figure of 12 dB for the estimated screening effectiveness of the box at this frequency.

---

The size of the box in the preceding example was chosen to be typical of the kind of enclosure commonly used for electronic equipment. The lowest resonant frequency is high enough to cause little trouble unless the circuit enclosed is a microwave circuit. However if the box were larger, or if the circuit were encapsulated in epoxy resin the frequency would come down into the region of operation of high-speed digital circuits. In that case the box would screen the circuit very imperfectly from external signals at the resonant frequency. In addition, if the resonance were excited by the operation of the circuit itself at either the fundamental or a harmonic frequency, there could be strong cross-coupling effects within the circuit. This is why circuit designers must have an understanding of electromagnetic theory.

For much larger enclosures such as screened rooms there will be many higher-order resonances close to typical operating frequencies of electronic circuits. It is therefore necessary to ensure that these resonances are excited as weakly as possible by equipment within the room.

## 7.5 DIELECTRIC RESONATORS

In Chapter 3 it was demonstrated that strips and rods of dielectric material can act as waveguides. It follows that isolated pieces of dielectric may be expected to behave as resonators. One simple way of making a dielectric resonator is to place a section of dielectric rod waveguide between two parallel conducting planes. These act as short circuits and the lowest resonant frequencies can be worked out if the dispersion curve for the waveguide can be measured or calculated. If the relative permittivity of the material is high then (3.4) shows that signal is strongly reflected at an air–dielectric interface. For example titanium dioxide has a relative

permittivity of 90 so the reflection coefficient of a TEM wave incident normally on the boundary from within the material is

$$\varrho = \frac{\sqrt{90} - 1}{\sqrt{90} + 1} = 0.81. \tag{7.58}$$

Thus it is possible to make a resonator out of such a material without any conducting boundaries. Note that (7.58) shows that the reflected wave is in phase with the incident wave so that, to a first approximation, the interface behaves as an open circuit. In order to achieve a reversal in the direction of the Poynting vector the direction of the magnetic field must be reversed at the boundary. That therefore behaves approximately as a magnetic short circuit or 'perfect magnetic conductor'.

If the approximation is made that the dielectric is bounded by a perfect magnetic conductor then the solution is obtained from that for a metallic resonant cavity by interchanging the roles of the electric and magnetic fields. In particular for a cylindrical piece of dielectric the lowest resonant mode has an axial magnetic field and a tangential electric field as shown in Fig. 7.15 by analogy with the pill-box cavity in Fig. 7.13. The frequency of this mode is then given by (7.49) with $k_0$ replaced by $k_1 = k_0\sqrt{\varepsilon_r}$, giving

$$f_{\mathrm{GHz}} = \frac{0.115}{r\sqrt{\varepsilon_r}}. \tag{7.59}$$

Thus a titanium dioxide resonator is smaller than a cavity resonator having the same resonant frequency by a factor of $\sqrt{90} = 9.5$. Dielectric resonators are therefore much more compact than corresponding cavity resonators. They can be made with low loss and therefore high $Q$ compared with microstrip resonators.

An important advantage of dielectric resonators is their temperature

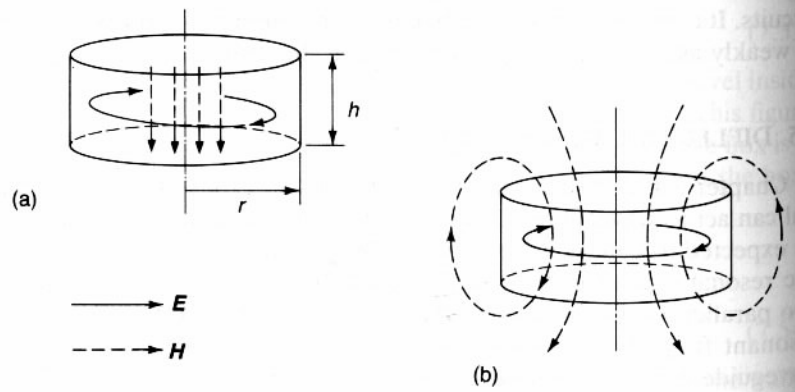


**Fig. 7.15** Dielectric resonators: (a) approximate fields, and (b) the correct field pattern.



stability. The frequency of a metallic cavity resonator decreases with increasing temperature as the cavity expands. Dielectric resonators likewise expand as the temperature increases but the relative permittivity is also frequency dependent. For a material such as barium nanotitanate the relative permittivity decreases with temperature at a rate which almost exactly compensates for the thermal expansion. This is particularly useful for making stable local oscillators and narrow band filters.

The theory given above can only be approximate because, as (7.58) shows, the assumption that the boundaries are perfect magnetic conductors is not strictly correct. A full theory must include the effects of the leakage fields outside the dielectric. These are two-fold. First they modify the resonant frequency and, secondly, they result in a loss of energy by radiation so lowering the $Q$ of the resonator. The field pattern around the resonator is, in practice, as shown in Fig. 7.15(b) so that it behaves as a magnetic dipole radiator. This is the mode commonly used in dielectric resonators. It is referred to as the $\mathrm{TE}_{01\delta}$ or 'magnetic dipole' mode. An empirical formula for the resonant frequency obtained from numerical solutions is (from Kajfez and Guillon, 1986)

$$f_{\mathrm{GHz}} = \frac{0.034}{r\sqrt{\varepsilon_r}}\left(\frac{r}{h} + 3.45\right). \tag{7.60}$$

This formula is accurate to within 2% for $0.5 < r/h < 2$ and relative permittivities in the range 30 to 50.

The $Q$ factor of an isolated dielectric resonator is about 50 because of radiation losses. If the resonator is placed within a conducting shield these losses are dramatically reduced and $Q$ factors around 5000 can be achieved. Because in a typical case 95% of the stored electric energy and over 60% of the stored magnetic energy are within the dielectric the resonant frequency is determined largely by the dielectric so it is insensitive to small changes in the dimensions of the shield.

The leakage of magnetic flux from the resonator provides a convenient way of coupling it to a microstrip line. Figure 7.16 shows a typical arrangement.

It must be remembered that a dielectric resonator like any other distributed resonator has an infinite set of resonant modes. Sometimes these can be troublesome. For example Fig. 7.17 shows a simple form of waveguide window. Windows are used to enable microwave power to pass from air into vacuum in vacuum electron devices. Simple transmission-line theory shows that the window shown will be transparent at the frequency at which it is half a wavelength in thickness. The dielectric would usually be alumina which has a relative permittivity of 8.9. Whilst this figure is not as high as those for materials designed for use as dielectric resonators it is still high enough for dielectric resonances to occur. The shielded arrangement of the dielectric means that these modes can have quite high $Q$ factors and be

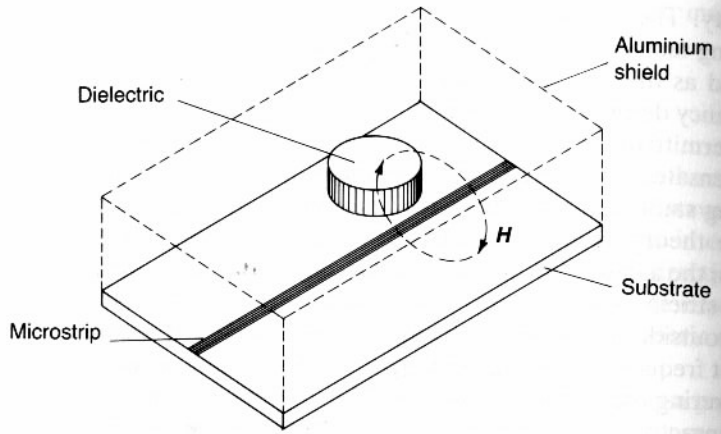


**Fig. 7.16** Coupling from a microstrip line to a dielectric resonator.

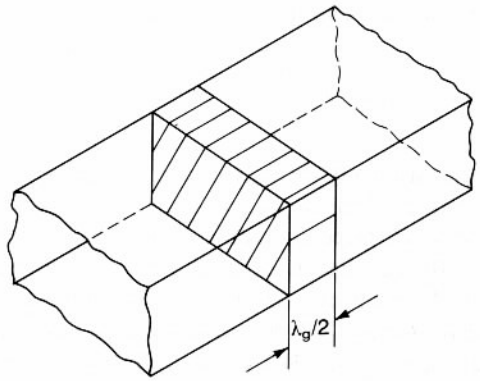


**Fig. 7.17** Half-wavelength waveguide window.

only weakly coupled to the wave in the waveguide. They are quite difficult to detect and are therefore known as 'ghost modes' (Forrer and Jaynes, 1960). If one of these modes occurs within the operating frequency band of the window appreciable power can be dissipated by it, thus giving rise to unwanted heating and possible destruction of the window.

## 7.6 FABRY–PÉROT RESONATORS

A particularly simple form of resonator for TEM waves can be made by arranging a pair of plane reflecting surfaces parallel to each other as shown in Fig. 7.18. This arrangement is known as a Fabry–Pérot resonator. Res-



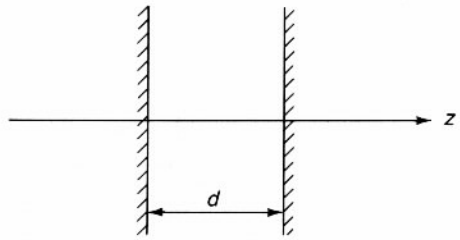


**Fig. 7.18** Fabry–Pérot resonator.

onance occurs when the waves are travelling normal to the surfaces and the condition for resonance is

$$d = n\lambda/2. \tag{7.61}$$

If the surfaces are made so that the reflection is not quite perfect then it is possible to couple power into and out of the resonator. At microwave frequencies this could be achieved by using wire grids or thin conducting films evaporated on to dielectric surfaces. The former arrangement provides the possibility of making resonators which select one polarization of the wave. At optical frequencies the partial reflection is achieved by the use of thin films.

Fabry–Pérot resonators are used in lasers and are also important as a way of making accurate optical filters.

## 7.7 FILTER THEORY

Resonators are important because of their ability to select and reject frequencies. This property finds particular application in the fabrication of filters. A filter is a device which passes a band of frequencies whilst blocking other frequencies. Figure 7.19 shows the idealized transfer functions of the four possible types of filter. These are respectively, low-pass, high-pass, band-pass and band-stop filters. Their uses include the suppression of harmonics and the selection of bands of frequencies in frequency-domain multiplex communication systems. The theory of filters including techniques for their synthesis is a major subject in its own right. Here we shall concentrate on the links between filter theory and the properties of transmission lines and resonators already discussed.

At low frequencies filters can be realized using lumped inductors and capacitors. Figure 7.20 shows examples of lumped-element low- and high-pass filter networks. The way in which these work can easily be understood if it is remembered that an inductor has an impedance which is zero for d.c. and which increases with frequency. Similarly, a capacitor provides a total block to d.c. but has a decreasing impedance as the frequency increases.

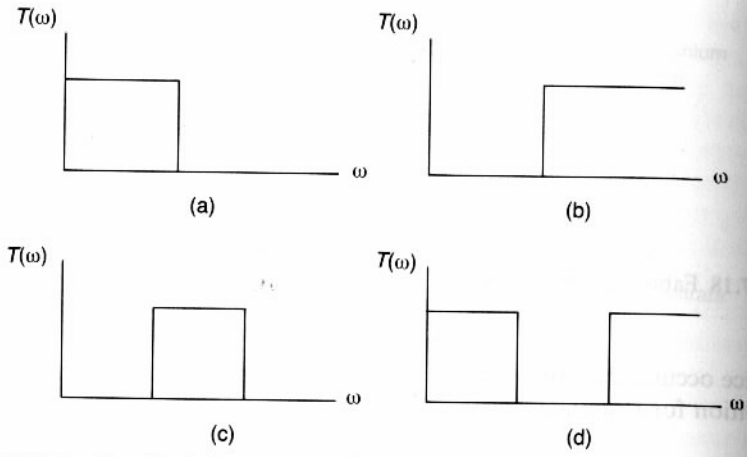


**Fig. 7.19** The four ideal filter characteristics: (a) low-pass, (b) high-pass, (c) band-pass, and (d) band-stop filters.

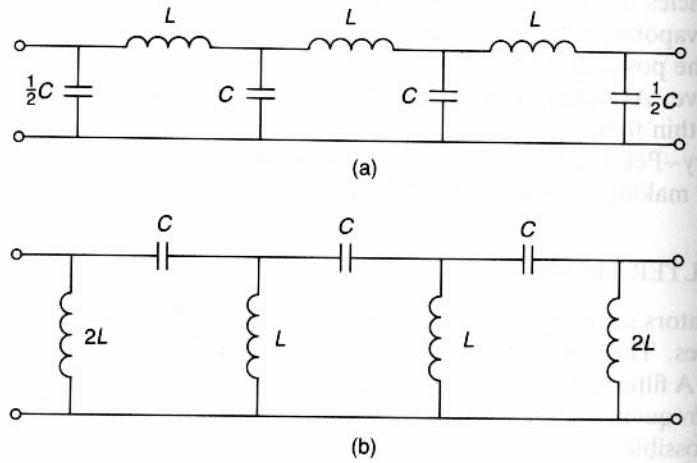


**Fig. 7.20** Filter networks: (a) low pass, and (b) high pass.

Thus the low-pass filter shown in Fig. 7.20(a) provides no obstacle to d.c. At high frequencies the passage of current is blocked by the inductors and a low impedance path to ground is provided by the capacitors. It can be shown (Jones and Hale, 1982) that the transfer function of the network shown in Fig. 7.20(a) can be designed to have the forms

$$|T(\omega)|^2 = \frac{1}{1 + k^2\left(\frac{\omega}{\omega_0}\right)^{2N}} \tag{7.62}$$



for a Butterworth response and

$$|T(\omega)|^2 = \frac{1}{1 + k^2 T_N^2\left(\frac{\omega}{\omega_0}\right)} \tag{7.63}$$

for a Tchebychev response by a suitable choice of the component values. In these expressions $k$ is a parameter which defines the minimum loss within the passband of the filter, $N$ is the number of components in the network, $T_N$ is the Tchebychev polynomial of order $N$ and $\omega_0$ is given by

$$\omega_0 = 1/\sqrt{(LC)}. \tag{7.64}$$

It is also necessary to ensure that the component values are chosen so that the filter is matched to the source impedance within its pass band.

A high-pass filter can be derived from a low-pass filter by the transformation

$$\frac{\omega}{\omega_0} \rightarrow -\frac{\omega_0}{\omega}. \tag{7.65}$$

Thus in Fig. 7.20 the series inductance $L$ in Fig. 7.20(a) transforms to

$$-\mathrm{j}\,\frac{\omega_0^2 L}{\omega} = \frac{1}{\mathrm{j}\omega C}, \tag{7.66}$$

where $C$ is the corresponding shunt capacitance in Fig. 7.20(b).

Figure 7.21 shows typical transfer characteristics for a pair of low- and high-pass filters designed in this way.

Band-pass and band-stop filters can also be derived from a low-pass filter by the transformations

$$\frac{\omega}{\omega_0} \rightarrow \frac{\omega_0}{\omega_2 - \omega_1}\left(\frac{\omega}{\omega_0} - \frac{\omega_0}{\omega}\right) \tag{7.67}$$

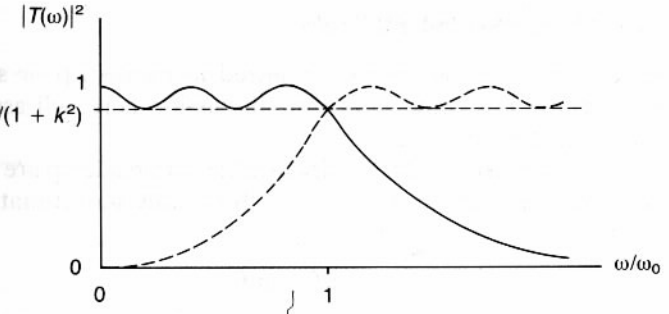


**Fig. 7.21** Transfer characteristics for low-pass and high-pass Tchebychev filters.

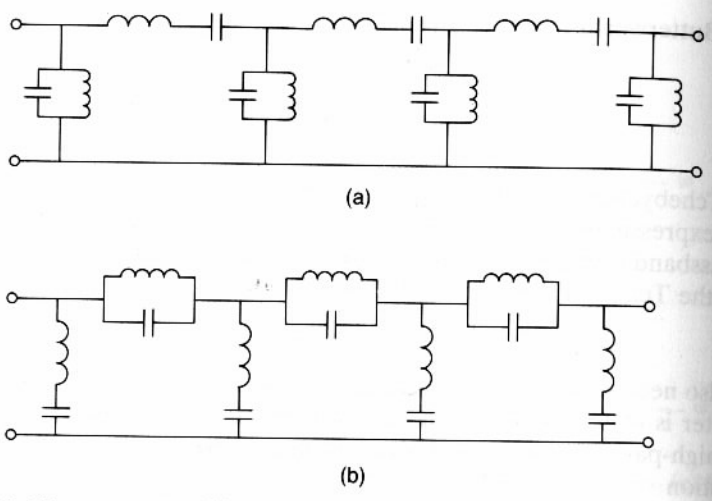


**Fig. 7.22** Filter networks: (a) band pass, and (b) band stop.

and
$$\frac{\omega}{\omega_0} \rightarrow \left[\frac{\omega_0}{\omega_2 - \omega_1}\left(\frac{\omega}{\omega_0} - \frac{\omega_0}{\omega}\right)\right]^{-1}, \tag{7.68}$$

where $\omega_1$ and $\omega_2$ are the upper and lower limits of the pass or stop band and $\omega_0 = \sqrt{(\omega_1\omega_2)}$. The second term in each of these expressions is familiar from equations (7.2) and (7.21) so it is not unexpected that these two filters incorporate resonant elements. It can be shown that the transformations replace the series inductors of the low-pass filter by a series resonant circuit and the capacitors by parallel resonant circuits to obtain the band-pass network shown in Fig. 7.22(a). Exchanging the series and shunt resonant circuits produces the band-stop network shown in Fig. 7.22(b). Once again it is possible to understand how these networks work if it is recalled that the shunt and series resonant circuits have maximum and minimum impedance respectively at resonance.

## 7.8 TRANSMISSION-LINE FILTERS

Transmission-line filters are usually realized in microstrip or suspended substrate stripline. For convenience the discussion here will assume that microstrip is being used.

The basic elements from which stripline filters are made up are the short- and open-circuit stubs shown in Fig. 7.23. It is easily shown that the input impedances are

$$Z = jZ_0 \tan\theta \tag{7.69}$$

for the short-circuit stub, where $\theta$ is the electrical length, and



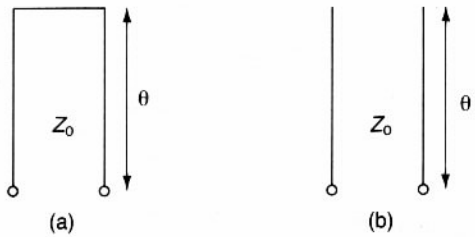


**Fig. 7.23** Transmission-line filter elements: (a) short-circuit stub, and (b) open-circuit stub.

$$Z = \frac{1}{jY_0 \tan\theta} \tag{7.70}$$

for the open-circuit stub. Thus the inductors and capacitors of the low-frequency networks can be replaced by short- and open-circuit stubs, respectively. Tan $\theta$, which is frequency dependent, takes the place of $\omega$. This produces one important difference between microwave filters and lumped-element filters. Tan $\theta$ is periodic in $\omega$ so there is a succession of frequencies at which a stub will behave as a short circuit or an open circuit. At intermediate frequencies the roles of the stubs are reversed. The result of this is that a low-pass network has a succession of higher-order pass bands with stop bands between them. Figure 7.24 shows the stripline analogue of the low-pass network shown in Fig. 7.20(a). The transfer factor of this filter is shown in Fig. 7.25. The filter shown in Fig. 7.24 is impossible to realize because of the difficulty of making the shunt stubs and because of the need to have a finite distance between the points at which the stubs are connected together. The solution to this problem is to make use of the impedance transformation properties of the main transmission line to allow all the elements to be open-circuit shunt stubs.

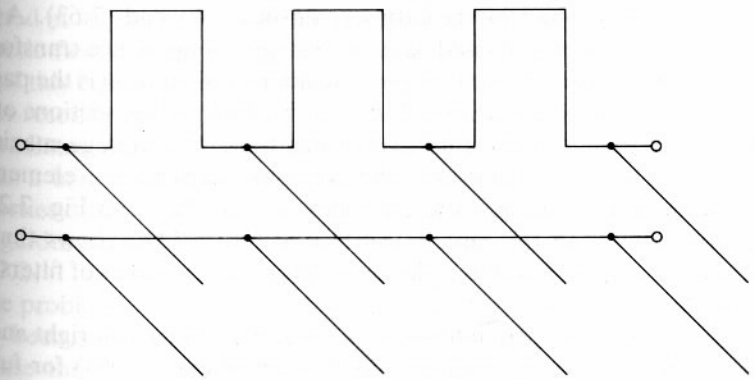

**Fig. 7.24** Stripline analogue of the low-pass filter network shown in Fig. 7.20(a).

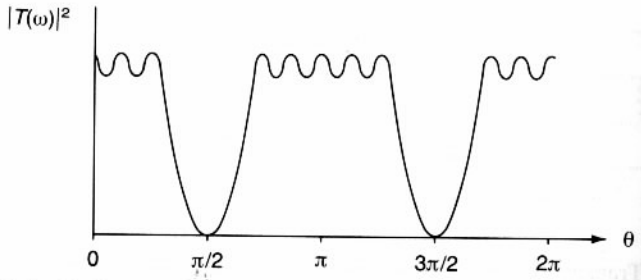


**Fig. 7.25** Periodic frequency response of a Tchebychev low-pass filter realized in stripline.

The theory of a simple filter comprizing a series of reflecting elements separated by equal electrical lengths θ can be understood by reference to the discussion of broadband matching in Section 6.7. There it was shown that, for small reflections, the reflection coefficient of the set of reflections $\varrho_1, \varrho_2, \varrho_2, \varrho_1$ could be written

$$|\varrho| = |8\varrho_1 x^3 + 2(\varrho_2 - 3\varrho_1)x| \tag{7.71}$$

(equation (6.3)) where $x = \cos\theta$. It was also shown that this could be put into the form of Butterworth or Tchebychev polynomials by a suitable choice of $\varrho_1$ and $\varrho_2$. Now the power reflected by this device is given by

$$P_r = |\varrho|^2 P_i \tag{7.72}$$

so the power transmitted is given by

$$\frac{P_t}{P_i} = 1 - |\varrho|^2$$

$$\simeq \frac{1}{1 + |\varrho|^2} \tag{7.73}$$

which can be expressed in the forms given in (7.62) and (7.63). A very similar result could be obtained by using a stepped impedance transformer as shown in Fig. 7.26(a). Another possible filter configuration is the parallel coupled band-pass filter shown in Fig. 7.26(b). Each of the sections of line behaves as a parallel resonant circuit since there is a voltage maximum at its ends when it is resonant. The coupling between the elements is capacitive so the device has the equivalent circuit shown in Fig. 7.26(c). Comparison between this circuit and that in Fig. 7.22(a) shows that the filter must be a band-pass filter. All these filters are examples of filters with periodic structures.

The design of microstrip filters is a major subject in its own right and the reader should refer to specialized texts (Matthaei *et al.*, 1964) for further information.



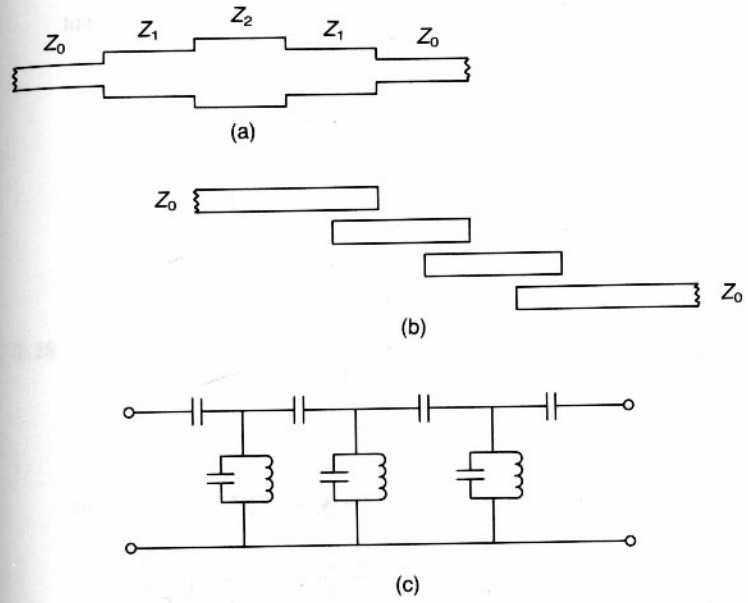


**Fig. 7.26** Microstrip filters: (a) stepped-impedance, and (b) parallel-coupled band-pass filters with (c) the equivalent circuit of the latter.

## 7.9 WAVEGUIDE FILTERS

At power levels above a few watts it is necessary to use waveguide technology to make filters. The approach used is essentially the same as in the case of transmission lines.

Figure 7.27(a) shows a section of waveguide with a resonant section formed by two transverse walls at A and B. These walls have small coupling irises in them. An incident wave in the waveguide is almost completely reflected at A producing a standing wave in the waveguide. The tangential magnetic field therefore induces a magnetic dipole in the iris at A. The field of this dipole at the iris at B is negligible unless the cavity is resonant. Under resonant conditions the field of the cavity excites the iris at B which then radiates power into the output waveguide. This arrangement therefore acts as a band-pass filter. Provided that the coupling irises are small the properties of the cavity are not affected by loading by the input and output waveguides and the transfer characteristic of the filter is essentially that of Fig. 7.2.

The problem with this kind of filter is that the transmission loss is rather large because of the bad mismatch at A. If the irises are enlarged to increase the coupling then the input and output guides load the cavity reducing its $Q$ factor and possibly tuning its resonant frequency.

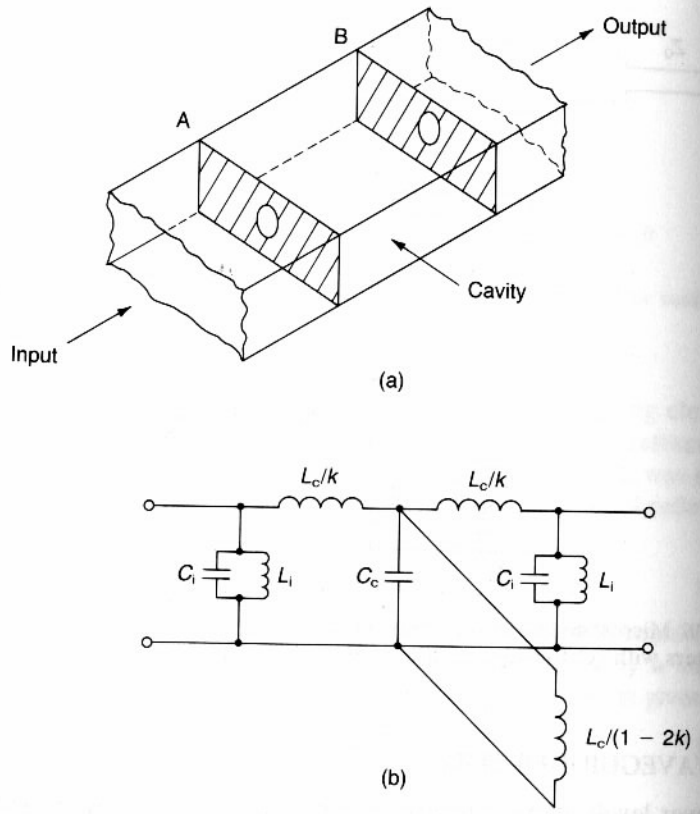


**Fig. 7.27** Iris-coupled waveguide band-pass filter: (a) general arrangement, and (b) equivalent circuit.

The equivalent circuit of the filter is shown in Fig. 7.27(b). The irises are represented by parallel $LC$ circuits because there is inductance associated with the flow of current around the hole and capacitance associated with the displacement current across it. The cavity inductance $L_c$ is divided into three parts because not all the circulating current in the cavity is intercepted by the irises. The resulting equivalent circuit clearly has a band-pass characteristic as can be seen by comparing it with Fig. 7.22(a).

In order to control the transfer characteristic of the filter several cavities may be connected in series as shown in Fig. 7.28. The behaviour of this arrangement can be understood by considering the extreme cases when the cavities are resonating in phase or in antiphase with each other. Figure 7.29 shows how this happens. In Fig. 7.29(a) the cavities are excited in phase with each other. The conduction currents in adjacent cavities are crossing the irises in the same directions. The irises being small are well below their lowest resonant frequency so they present an inductance to the current.



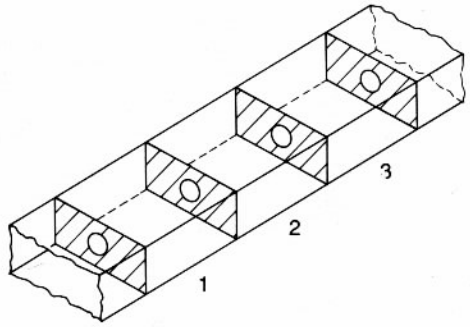


**Fig. 7.28** Multi-cavity waveguide band-pass filter.

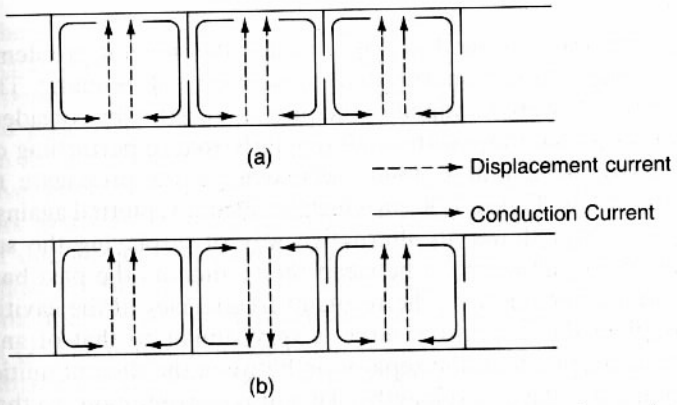


**Fig. 7.29** Conduction and displacement currents in the filter shown in Fig. 7.28 (a) at zero phase shift per section, and (b) at 180° phase shift per section.

This inductance is in series with the cavity inductance so it has the effect of lowering the resonant frequency a little. When the cavities are excited in antiphase (Fig. 7.29(b)) the conduction currents flow across the irises in opposite directions. There is, therefore, no net current flow across each iris and the resonant frequency is unperturbed. For other possible phase changes there is an intermediate situation so the in-phase and anti-phase conditions represent the edges of a band of frequencies which the filter will pass. Careful design of the sizes of the irises and of the resonant frequencies of the cavities can produce either Butterworth or Tchebychev characteristics in the pass band.

The filter shown in Fig. 7.28 also has a series of higher-order pass bands corresponding to those higher-order modes of the cavities which couple to the irises. Thus a filter comprising a series of weakly coupled cavities has narrow pass bands separated by broad stop bands. In describing the action

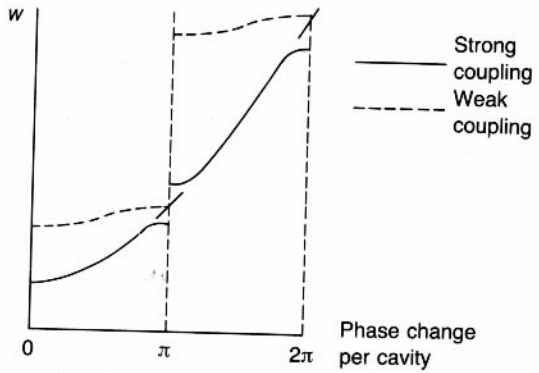


**Fig. 7.30** The dispersion diagram of the filter shown in Fig. 7.28.

of the filter in this way we have approached the general problem of the coupled resonator filter from the point of view of weak coupling. The same qualitative results were obtained in the previous section by considering the case of a transmission line with small regularly spaced perturbing objects.

This kind of behaviour is found whenever waves propagate through periodic structures. Figure 7.30 (in which frequency is plotted against phase change per cavity) shows an alternative way of displaying the same information. For weak coupling between the resonators the pass bands are narrow and are very close to the resonant frequencies of the cavities. For strong coupling the dispersion curve is very similar to that of an empty waveguide expcept where the separation between the discontinuities is an integral number of half wavelengths. Then it is discontinuous so that there is a stop band.

This discontinuity can be explained by considering Fig. 7.31 which shows the electric and magnetic fields in the waveguide when the separation of the obstacles is a half wavelength. The cumulative reflections set up a standing wave in the guide and any general standing wave can be regarded as the superposition of the two 'normal modes' shown in the figure. In Fig.

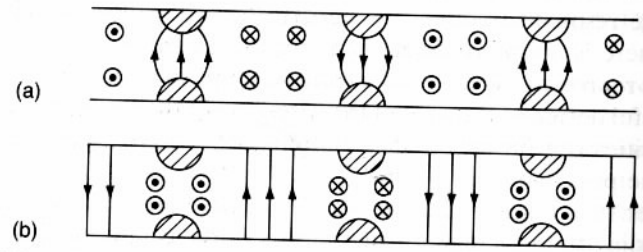


**Fig. 7.31** Fields in the filter shown in Fig. 7.28 at the two edges of the stop band when the phase change per section is 180°.



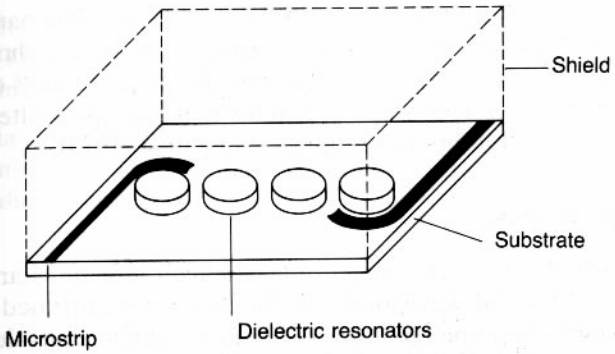


**Fig. 7.32** Band-pass filter using dielectric resonators.

7.31(a) the electric field maxima coincide with the obstacles. For this mode the capacitance is reduced and the frequency is slightly higher than in the unperturbed mode. In the second case (Fig. 7.31(b)) the magnetic field is perturbed producing an increase in the effective inductance and a slight reduction in the resonant frequency.

We have therefore demonstrated, both from the point of view of coupled resonators and from that of perturbed waveguide modes, that periodic arrays of discontinuities in a waveguide produce alternate pass and stop bands whose widths depend upon the magnitudes of the discontinuities.

Stripline filters have the disadvantage that it is difficult to get very high values of $Q$. The theoretical behaviour is therefore limited by the inherent bandwidths of the elements from which the filter is made up. One solution to this is to make use of dielectric resonators as shown in Fig. 7.32. The resonators are inductively coupled just like the cavities in Fig. 7.28. The filter has a band-pass characteristic.

## 7.10 OPTICAL FILTERS

At optical frequencies filters can be made by using Fabry–Pérot resonators. A series of layers of transparent dielectric separated by thin metallic films or by layers of a different dielectric has the equivalent circuit shown in

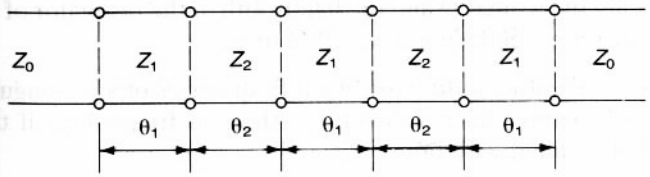


**Fig. 7.33** Equivalent circuit for an optical filter employing layers of different dielectric materials.

Fig. 7.33. This periodic structure has alternate pass and stop bands exactly like those discussed in the preceding sections. By careful choice of the filter dimensions it is possible to ensure that all the pass bands except one lie outside the visible spectrum. This filter is a band-pass filter. Further details can be found in books on optics (Longhurst, 1973).

## 7.11 CONCLUSION

In this chapter we have considered how resonant structures are made in transmission lines and waveguides. It has been demonstrated that such structures can be described in terms of lumped-element equivalent circuits with the difference that distributed structures can support infinite sets of higher-order resonant modes. Resonant circuits are important because of their frequency-selective properties. These can be enhanced by combining resonant circuits into filter structures. The four basic filter types (low pass, high pass, band pass and band stop) can all be derived from a low-pass filter. Filters can be designed in both transmission lines and waveguides from lumped-component, low-frequency, models. Certain changes are necessary in order to adapt the designs to the particular technology in which they are to be realized.

Most filters have a periodic structure and exhibit alternate pass and stop bands. The pass bands get wider as the strength of the coupling between the elements of the filter increases. This behaviour can be understood either by considering the perturbation of waves by regularly spaced discontinuities or by considering the behaviour of weakly coupled resonators.

## EXERCISES

**7.1** Calculate the equivalent circuit parameters for a microwave cavity which resonates at 3.40 GHz with a $Q$ of 600 and an $R/Q$ of 450 Ω. Find the amplitude and phase of its impedance at 3.38 GHz and 3.43 GHz.

**7.2** Calculate the lowest three resonant frequencies of a 75 Ω semi-airspaced, coaxial cable ($\varepsilon_r = 1.06$) used as the downlead from a television antenna if the cable is 15 m long.

**7.3** Calculate the loaded $Q$ and the bandwidth of the resonator of Question 7.1 when it is connected to a 10 kΩ load.

**7.4** Calculate the lowest three resonant frequencies of a rectangular cavity 17 mm × 21 mm × 12 mm. What are the new frequencies if the box is completely filled with epoxy resin ($\varepsilon_r = 3.5$)?

**7.5** A rectangular metal box 510 mm × 550 mm × 126 mm which has a screening effectiveness of 120 dB is illuminated uniformly by an electromagnetic wave having a power density of 1 mW m$^{-1}$ at the frequency of the lowest resonance of the box. If the $Q$ factor of the resonance is 90 estimate the screening effectiveness at this frequency.



**7.6** Calculate the dimensions of a pill-box dielectric resonator made of barium titanate ($\varepsilon_r = 1200$) if the resonant frequency is 9.5 GHz and the radius is twice the height.